ELSEVIER

Compositional changes of a dicalcium phosphate dihydrate cement after implantation in sheep

M. Bohner[a],*, F. Theiss[b], D. Apelt[b], W. Hirsiger[a], R. Houriet[c], G. Rizzoli[d], E. Gnos[e], C. Frei[f], J.A. Auer[b], B. von Rechenberg[b]

[a] *Dr h.c. Robert Mathys Foundation, Bischmattstr 12, CH-2544 Bettlach, Switzerland*
[b] *MSRU, Department of Veterinary Surgery, University of Zurich, Winterthurerstr. 260, CH-8057 Zurich, Switzerland*
[c] *Laboratory of Powder Technology, Ecole polytechnique Fédérale de Lausanne, CH-1015 Lausanne, Switzerland*
[d] *Mathys Medical, Güterstr 5, CH-2544 Bettlach, Switzerland*
[e] *Institute of Geological Sciences, University of Bern, Baltzerstr. 1-3, CH-3012 Bern, Switzerland*
[f] *Stratec Medical, Eimattstrasse, CH-4436 Oberdorf, Switzerland*

Abstract

A hydraulic calcium phosphate cement having dicalcium phosphate dihydrate (DCPD) as end-product of the setting reaction was implanted in a cylindrical defect in the diaphysis of sheep for up to 6 months. The composition of the cement was investigated as a function of time. After setting, the cement composition consisted essentially of a mixture of DCPD and β-tricalcium phosphate (β-TCP). In the first few weeks of implantation, the edges of the cement samples became depleted in DCPD, suggesting a selective dissolution of DCPD, possibly due to low pH conditions. The cement resorption at this stage was high. After 8 weeks, the resorption rate slowed down. Simultaneously, a change of the color and density of the cement center was observed. These changes were due to the conversion of DCPD into a poorly crystalline apatite. Precipitation started after 6–8 weeks and progressed rapidly. At 9 weeks, the colored central zone reached its maximal size. The fraction of β-TCP in the cement was constant at all time. Therefore, this study demonstrates that the resorption rate of DCPD cement is more pronounced as long as DCPD is not transformed in vivo.
© 2003 Elsevier Science Ltd. All rights reserved.

Keywords: Brushite; Cement; In vivo test; Apatite

1. Introduction

In the last two decades, there has been a growing interest for calcium phosphate cements (CPC) [1–3]. CPC are excellent bone substitutes: they are biocompatible, resorbable and easy to handle [4–6]. CPC are obtained by mixing one or several calcium phosphate powders with an aqueous solution. Upon mixing, the calcium phosphate powders dissolve, and new calcium phosphate crystals form. The entanglement of these crystals results in paste hardening.

There are two types of hydraulic CPC depending on the end-product of the reaction: apatite cements and dicalcium phosphate dihydrate (DCPD) cements (CaHPO$_4 \cdot$2H$_2$O) [4–6]. Most studies have been devoted to

apatite cements due to three main reasons: (i) apatite is the calcium phosphate phase present in bone; (ii) apatite cements are mechanically more favorable; and (iii) contrary to DCPD cements, apatite cements set at neutral pH values. Despite these advantages, DCPD cements have raised a large interest [3,5,6]. DCPD is a metastable calcium phosphate phase in physiological conditions [7]. Therefore, DCPD cements are much faster resorbable than apatite cements [8,9].

In a recent study in sheep [10], the resorption rate of a particular DCPD cement was observed to be slow. Simultaneously, an apatite phase was detected in the cement implant, suggesting the in vivo transformation of DCPD into apatite [11]. The transformation of a DCPD cement into apatite was also observed in a rabbit study [12].

Clearly, a fast resorption of DCPD cements can only be achieved if the cement resorption occurs before the cement conversion. Thus, an attempt was made to

prevent the in vivo transformation by adding an inhibitor of apatite crystal growth. For that purpose, a poorly soluble magnesium salt was added to the cement formulation [13]. This concept was tested in vitro and proved to work: small amounts of magnesium prevented the transformation of DCPD into an apatite [14].

Recently, magnesium-containing DCPD cements were implanted in vivo. Results showed that the resorption of these DCPD cements was much faster than that of a carbonated apatite cement [15–17]. The resorption rate decreased very rapidly with time, especially beyond 8 weeks of implantation (Fig. 1) [15–17]. After 6–8 weeks of implantation, a change of coloration appeared in the center of the cement implants. This color change was particularly visible in the histological sections (Fig. 2). Initially, the cement colored with toluidine blue was blue. The granules had a slightly lighter blue color. After 6–8 weeks, the color of the center of the cement changed towards violet-purple. This darker zone was often surrounded by a rather pale thin layer (Fig. 2). This change in color suggested a change of cement composition, or a change of the local
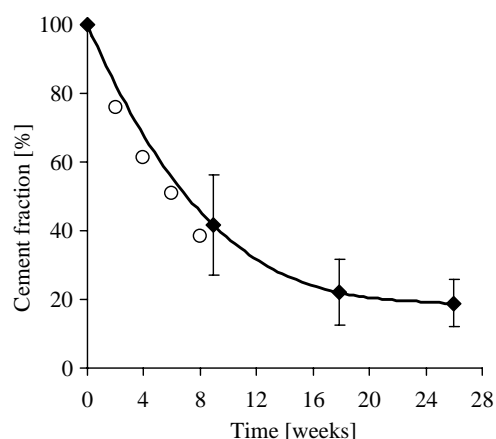
pH value. As the conversion of DCPD cement into an apatite is not desired in terms of resorption rate, it was very important to determine whether this change of coloration was due to the precipitation of apatite. The goal of this article is to describe the evolution of the cement composition after implantation, and to correlate the cement resorption rate with its composition.

2. Materials and methods

The cement investigated here corresponds to the composition of chronOS Inject™ (Mathys Medical and Stratec Medical, Switzerland). The dry component of this cement consisted of 42 wt% β-TCP powder, 21 wt% MCPM, 31 wt% β-TCP granules, 5 wt% magnesium hydrogen phosphate trihydrate and small additions (<1 wt%) of sodium hydrogen pyrophosphate and magnesium sulfate to control the setting time. The liquid component consisted of a 0.5% solution of sodium hyaluronate. β-tricalcium phosphate (β-TCP; β-Ca$_3$(PO$_4$)$_2$), magnesium hydrogen phosphate trihydrate, sodium hydrogen pyrophosphate and magnesium sulfate were all purchased from Fluka (Buchs, Switzerland). Monocalcium phosphate monohydrate (MCPM; CaH$_2$PO$_4$)$_2$ · H$_2$O) was purchased from Albright–Wilson (West Midlands, UK). The sodium hyaluronate solution came from Vitrolife (Edinburgh, UK). The β-TCP granules were obtained by granulation of the β-TCP powder. The granules had an average diameter smaller than 0.5 mm and a theoretical density close to 75%. The cement set via the reaction

$$\beta\text{-Ca}_3(\text{PO}_4)_2 + \text{Ca}(\text{H}_2\text{PO}_4)_2 \cdot \text{H}_2\text{O} + 7\text{H}_2\text{O}$$
$$\rightarrow 4\text{CaHPO}_4 \cdot 2\text{H}_2\text{O}. \tag{1}$$

After setting, the cement was biphasic, i.e. it consisted of large granules of β-TCP (<0.5 mm in diameter) embedded in a matrix containing fine DCPD crystals and remnants of β-TCP powder (Fig. 2). According to reaction (1), the cement should contain about 55 wt% DCPD, 15 wt% β-TCP powder and 30 wt% β-TCP

Fig. 1. DCPD cement resorption as a function of implantation time. Cylindrical holes, 8 mm in diameter. (◆) First in vivo study [15,16]; (○) second in vivo study [17].
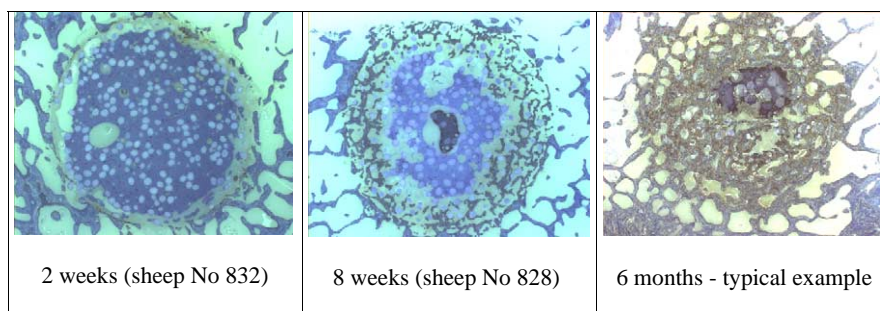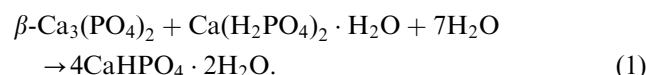

Fig. 2. Histological cross-sections of the cement after 2 weeks, 8 weeks, and 6 months implantation. The cylindrical holes have a diameter of 8 mm. The open structures present around the cement implants are trabecular bone (dark: bone mineral; light: marrow). The β-TCP granules present in the cement are seen as round pale spots. A change of coloration can be seen in the center of samples 828 (8 weeks) and 830 (6 months).

granules after setting (neglecting water, the pyrophosphate salt, and the magnesium salts). The porosity of the matrix and the granules was close to 35 vol%. The setting time of the cement at room temperature was 12 ± 2 min.

The cement samples were harvested from two different in vivo studies performed in sheep [15–17]. In the first study [15,16], two standardized drill holes of 8 mm in diameter and 13 mm in length were made bilaterally in the distal and proximal humerus and femur. In each sheep, three bone holes were filled with the brushite cement considered here and with an experimental DCPD cement, one hole was left empty as negative, and one hole was filled with Norian SRS (Norian Corporation, Cupertino, CA, USA) as positive control. The position of the different CPC and the control was randomized. A total of six sheep were used. Two sheep each were sacrificed after 2, 4 and 6 months. In the second study [17], a standardized drill hole of 8 mm in diameter and 13 mm in length was made unilaterally. Each hole was filled with the brushite cement considered here. Eight adult Swiss Alpine sheep served as experimental animals and were divided into four groups with two animals each. The study period until sacrifice of animals was 2, 4, 6 and 8 weeks. Radiographs were made immediately postoperatively and microradiographs at the time of sacrifice. After sacrifice, the bone samples were immediately harvested, macroscopically assessed and processed for histology. Non-decalcified bone specimens were embedded in acrylic resin (HistoDur®). Ground- (30–40 µm) and thin (5 µm) sections were prepared, and stained with either toluidine blue or "von Kossa/McNeal". Cross- and longitudinal sections of the cement samples were prepared, starting from the center of the sample (Fig. 3).

As the number of implantation sites was limited, the determination of the cement composition was performed on histological sections. Obviously, the treatments sustained by the cement samples in order to obtain histological sections might have affected the cement composition. As DCPD is only metastable at physiological pH, DCPD could transform into an apatite, octocalcium phosphate (OCP), or dicalcium phosphate (DCP). However, as all the processing steps were performed in a non-aqueous environment, the risk was low. The results presented hereafter suggest indeed that the composition of the cement was not modified by the processing steps: all cement samples implanted for a short time contained DCPD, whereas no DCP, OCP, and apatite were detected. Only the histological cross-sections were used for analysis. The first two series of cross-sections (starting from the sample center; Fig. 3) were used for histomorphometrical measurements and colored with toluidine blue. The third cross-sections were used for X-ray diffraction (XRD). Finally, the fourth cross-sections of the second in vivo study were used for
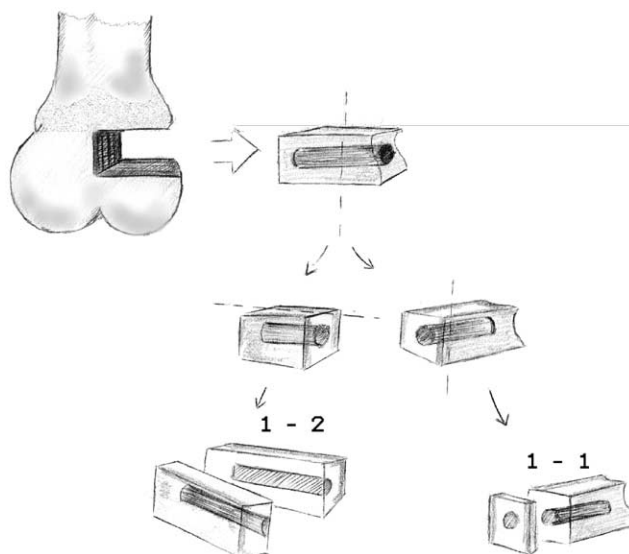

Fig. 3. Schema describing how the histological sections were cut. Left: longitudinal sections; right: cross-sections. The numbers shown on the schema are used to label the histological sections.

Fourier-transformed infrared spectroscopy (FTIR), scanning electron microscopy (SEM) equipped with an energy-dispersive X-ray (EDX), electron microprobe analyzer equipped with a wavelength dispersive spectrometer (WDS), micro-X-ray fluorescence (mXRF), and micro-Raman (Table 1). The last method did not enable the detection of DCPD. mXRF did not reveal more information than FTIR and was abandoned.

All histological sections of the first and second in vivo study were analyzed by XRD. To determine the cement composition before implantation, the cement remaining in the syringe (second in vivo study) was dried in air, ground in a mortar with a pestle, and analyzed. In each of the histological sections where cement was found, it was carefully cut off and ground per hand with a pestle and a mortar. This cement powder was homogenized and analyzed on a Si-single-crystal plate. Orientation of the particles could therefore not be excluded. The measurements were done on a Philips PW1800 X-ray powder diffractometer (XRD) using Cu-Kα radiation (40 kV, 30 mA) and an automatic divergence slit. The investigation range was from $4°$ to $40°$ (2θ) with 1 s per step ($0.02°$ 2θ).

The identification of the various crystallographic phases was difficult for two main reasons. First, many calcium phosphate compounds have peaks at identical positions which prevent a precise identification of the phases. Second, a low-crystalline phase was found with a large peak close to $d = 2.81$ Å, which corresponds to the 100% peak of pure hydroxyapatite (HA; $Ca_{10}(PO_4)_6(OH)_2$). However, the latter peak was often seen at a slightly lower d-value (typically 2.78–2.79) suggesting the presence of ionic substitutions [18]. The nature of these substitutions can only be assumed,

Table 1
Overview of the use of histological sections for analysis in the second sheep study

Sheep	Cross-section no.			
	1	2	3	4
832 (2 weeks)	Histology	Histology	XRD	SEM, EDX
833 (2 weeks)	Histology	Histology	XRD	
826 (4 weeks)	Histology	Histology	XRD	SEM, EDX
831 (4 weeks)	Histology	Histology	XRD	
829 (6 weeks)	Histology	Histology	XRD	
830 (6 weeks)	Histology	Histology	XRD	FTIR, SEM, EDX, μXRF
827 (8 weeks)	Histology	Histology	XRD	μRaman
828 (8 weeks)	Histology	Histology	XRD	FTIR, SEM, EDX, μXRF, WDS

In the first in vivo study (2 sheep at 2, 4, and 6 months), the first and second sections were used for histologies, whereas the third sections were used for XRD.

e.g. sodium, magnesium, carbonates, hydrogenophosphate, but none of these could be demonstrated. Apart from an apatite, the following phases were identified in the histological cuts: β-TCP, DCPD, DCP (CaHPO$_4$), and β-calcium pyrophosphate (β-CPP; β-Ca$_2$P$_2$O$_7$).

These phases have their maximum peaks at $d = 2.88\,\text{Å}$ (β-TCP; $2\theta = 31.1°$), $4.24/7.62\,\text{Å}$ (DCPD; $2\theta = 21.0°$ and $11.6°$, respectively), $2.96\,\text{Å}$ (DCP; $2\theta = 30.2°$), $3.02\,\text{Å}$ (β-CPP; $2\theta = 29.6°$) and around $2.81\,\text{Å}$ for the apatite (Standard files JCPDS 9-169, 9-77, 9-80, 33-297, 9-432; d is the lattice spacing). As previously mentioned, many of these compounds have peaks at identical positions. The problem is particularly acute for DCP, β-CPP and HA which were all probably present in small amounts in the cement samples. An additional problem was the fact that the apatite present in the cement was nanocrystalline, hence leading to very low and broad peaks. Therefore, the surface area of the peaks, S_d, at $d = 6.74\,\text{Å}$ (DCP, 14%; $2\theta = 13.1°$), $4.24\,\text{Å}$ (DCPD, 100%; $2\theta = 21.0°$), $3.09\,\text{Å}$ (β-CPP, 54%; DCP, 6%; $2\theta = 28.9°$), $2.88\,\text{Å}$ (β-TCP, 100%; $2\theta = 31.1°$), and $2.81\,\text{Å}$ (HA, 100%; β-CPP, 27%; $2\theta = 32.2°$) was determined using XRD-software "MacDiff", version 4.0.6 [19]. The amount of each phase, $A(x)$, was estimated according to

$$A(\beta - \text{TCP}) = S_{2.88}, \qquad (2)$$

$$A(\text{DCPD}) = S_{4.24}, \qquad (3)$$

$$A(\text{DCP}) = \frac{S_{6.74}}{0.14}, \qquad (4)$$

$$A(\beta - \text{CPP}) = \frac{1}{0.54}\left(S_{3.09} - \frac{S_{6.74}}{0.14}0.06\right), \qquad (5)$$

$$A(\text{HA}) = \left(S_{2.81} - \frac{S_{3.09}}{0.54}0.27\right). \qquad (6)$$

Based on the estimated amounts of each phase, the fraction of each phase could be easily determined:

$$F(x) = \frac{A(x)}{A(\beta - \text{TCP}) + A(\text{DCPD}) + A(\text{DCP}) + A(\beta - \text{CPP}) + A(\text{HA})}, \qquad (7)$$

where $F(x)$ was the fraction of the phase "x". Two remarks should be made on the validity of the XRD method: (i) these fractions give only qualitative results because no calibration was done; (ii) it was implied that the mass absorption coefficient was the same for each phase.

Two histological sections were analyzed with a FTIR spectrometer (Nicolet 510). They were extracted from the 6- and 8-week sheep (Table 1). The measurements were done on an ATR-diamond (Golden Gate) device. The investigated areas had a diameter of 0.6 mm and a depth of 2 μm. For each measurement, 128 scans were accumulated in order to increase the signal/noise ratio. The composition of the sample was measured along a line crossing the sample and the colored center. One measurement was done per millimeter. The bands at 567, 940, and 970 cm^{-1} were used to detect the presence of hydroxyapatite (HA), β-tricalcium phosphate (β-TCP), and brushite (DCPD).

Four different histological sections were analyzed by SEM and EDX, i.e. the sections of sheep 832 (2 weeks), 826 (4 weeks), 830 (6 weeks), and 828 (8 weeks) (Table 1). The latter two sections were also analyzed by FTIR (see above). The histological sections were first coated with carbon. They were then observed by SEM (Cambridge S360). Finally, a certain number of points were analyzed by EDX (Link Oxford Pentafet device coupled to an INCA software) to determine their atomic composition. Three different areas were analyzed: (i) the edge of the cement sample where no apparent

resorption was seen, (ii) the center of the cement sample (2–3 mm in diameter), and (iii) the colored area in the center of the sample (only present in sample 828 and 830; Fig. 2). Over 15 points were selected in each area, far from the β-TCP granules.

For WDS, microprobe analyses of sample 828 (8 weeks; Table 1) were obtained on a Cameca SX-50 microprobe using synthetic apatite and feldspar as mineral standards, WDS, and beam conditions of 15 kV, 20 nA, and 15 µm spot size. Data were reduced using the PAP procedure [20]. Totals were low because the phosphate material contained additions of organic compounds. Both WDS and EDX results were used to compare the composition within a sample and not between several samples. Moreover, the results were considered to be qualitative and not quantitative.

3. Results

Diffraction peaks could be easily detected on the XRD diffraction spectra (Fig. 4). However, the noise increased with an increase of the implantation time,

because the amount of cement that could be extracted decreased due to cement resorption. Based on the diffraction peaks, the fraction of each phase was estimated using Eqs. (2)–(7). At time zero, the cement samples contained β-TCP, DCPD, β-calcium pyrophosphate (β-CPP), and sometimes DCP (Figs. 4 and 5). After implantation, no DCP was detected (Fig. 5). The β-TCP and CPP fractions were stable over time, whereas that of DCPD decreased. Interestingly, the ratio of the intensity of the DCPD and β-TCP peaks was much lower in the histological sections than at time zero. The decrease of DCPD over time was compensated by the appearance of a peak around $d = 0.278 - 0.279$ nm, probably corresponding to an apatite (Fig. 5).

DCPD and β-TCP were observed by FTIR in the histological sections, contrary to hydroxyapatite. The height of the absorption peaks of β-TCP and DCPD reached a maximum in the center of the cement sample (Fig. 6). Interestingly, the ratio between the height of the absorbance peaks of DCPD and β-TCP presented a maximum in the center of the cement sample (Fig. 7). Assuming that the amount of DCPD and β-TCP was proportional to the height of the absorbance peaks,
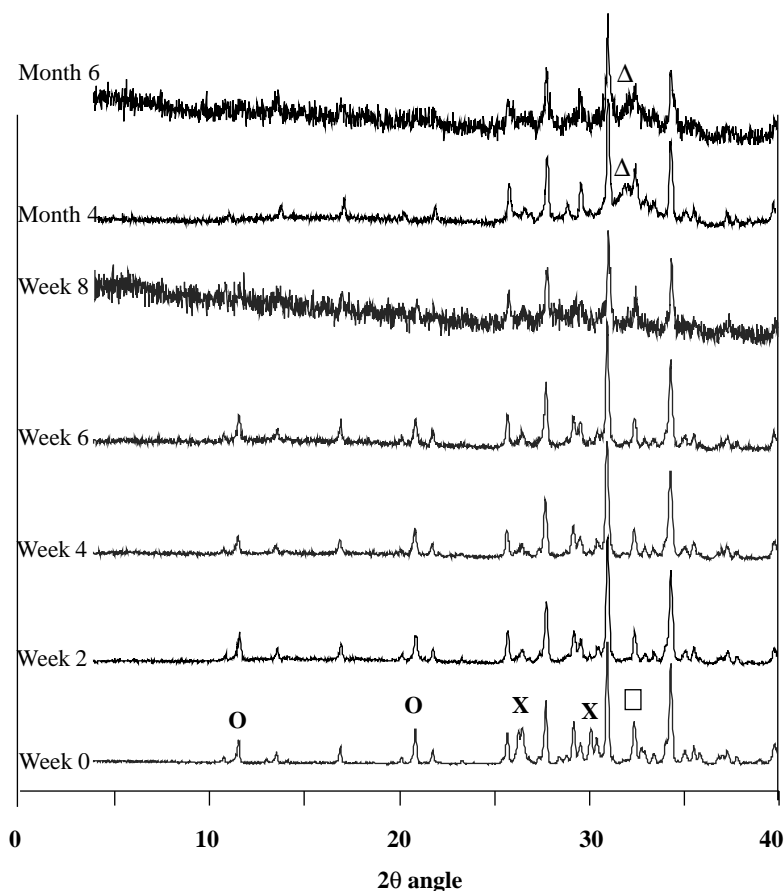

Fig. 4. XRD spectra of histological sections retrieved from sheep. Implantation time: 2, 4, 6, and 8 weeks, as well as 4 and 6 months. There is one spectrum represented per time, and the curves are in successive order, from bottom to top. The two main diffraction peaks of DCPD are indicated by a circle. The main diffraction peaks of DCP are indicated by a cross ($\times$). The apatite peak is represented with a triangle ($\triangle$). All the other major peaks are β-TCP diffraction peaks. One of the latter peaks which is present at $d = 2.757$ is marked with a square ($\square$).
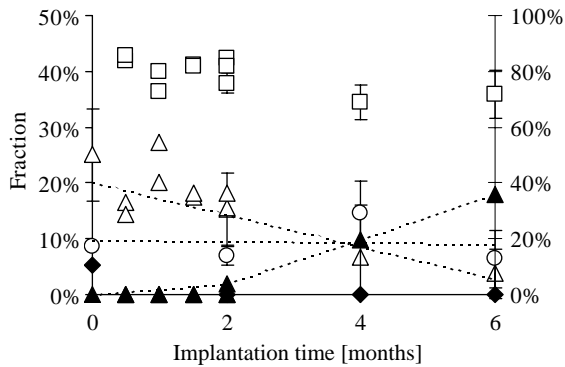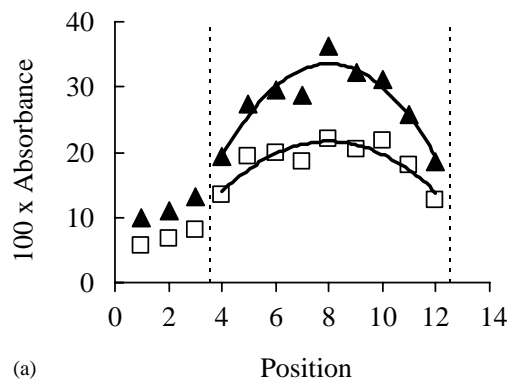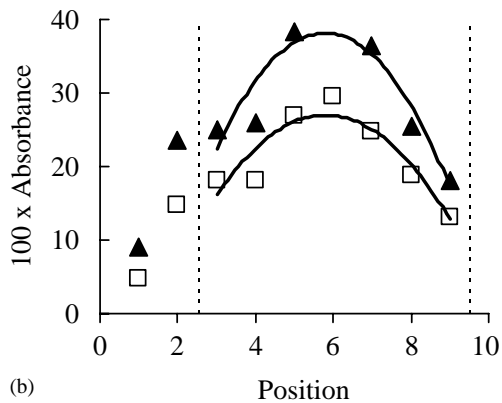
Fig. 5. Fractions of crystalline phases in the cement determined by comparing the surface area of the diffraction peaks. The error bars indicate 1.96 standard errors. ($\triangle$) DCPD (refers to the left axis); ($\blacklozenge$) DCP (left axis); ($\square$) β-TCP (right axis); ($\bigcirc$) β-CPP (left axis); and ($\blacktriangle$) HA (left axis).
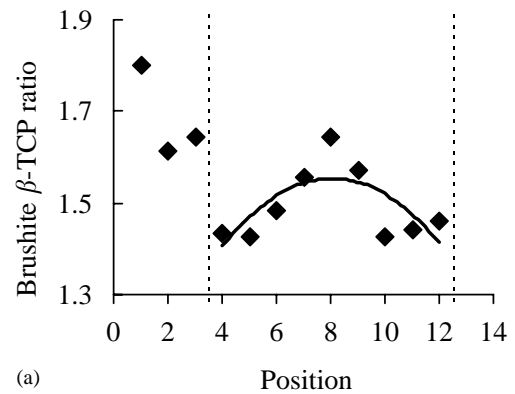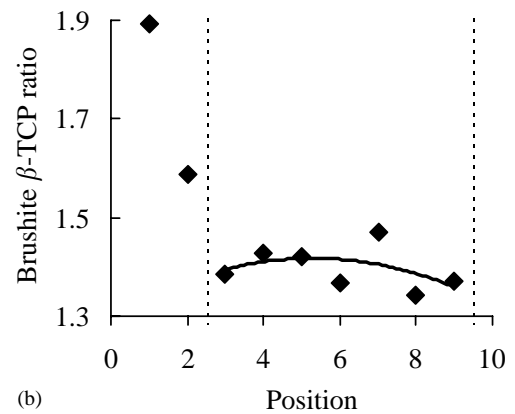

Fig. 6. Compositional changes across a cement sample obtained from FTIR measurements. (a) Sample 830 (6 weeks); (b) Sample 828 (8 weeks). Components: ($\square$) β-tricalcium phosphate, $940\,cm^{-1}$; ($\blacktriangle$) DCPD, $970\,cm^{-1}$. The dotted lines mark the limits of the cement implant. One measurement was done per millimeter.

these results indicate that (i) the cement sample was denser in its center than at its edges (Fig. 6), and (ii) DCPD concentration was lower at the cement edges than in the cement center (Fig. 7).

The microstructure of the cement was difficult to observe on the SEM machine used here due to the fact

Fig. 7. DCPD/β-TCP ratio across a cement sample obtained from FTIR measurements: (a) sample 830 (6 weeks) and (b) sample 828 (8 weeks). The dotted lines mark the limits of the cement implant.

that the samples were embedded in a polymer matrix. However, the colored center of the cement could be easily distinguished (Fig. 8). Moreover, this scan showed on the one hand that the colored center was surrounded by a porous zone, and on the other hand that the edge of the colored center was much denser than the rest of the colored center. A closer look at the cement micro-structure showed that the cement located close to the bone–cement interface contained a mixture of smooth and sharp particles (Fig. 9a). The angular particles had the typical shape of DCPD crystals [21]. In the porous zone, only smooth particles could be seen (Fig. 9b). In the so-called dense zone, the smooth particles were surrounded by a dense homogeneous layer (Fig. 9c). Finally, in the center of the colored zone, smooth particles were surrounded by small and sharp particles (Fig. 9d).

Using the EDX measurements, the Ca/P molar ratio and the Ca/C weight ratio were calculated for the different areas of the histological sections (Fig. 10). Variations of the Ca/P molar ratio were found to depend on the location. For example, the Ca/P molar ratio was significantly higher on the cement edge than in the center: $p < 0.0006$, 0.12, and 0.005 for samples
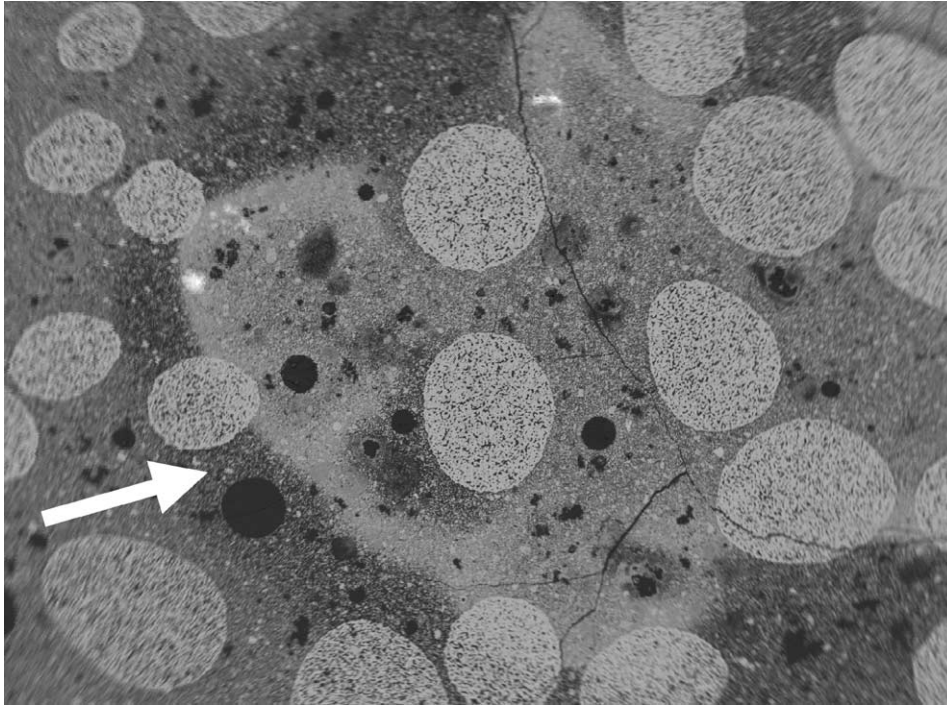
Fig. 8. Back-scattered electron image showing the colored center of sample 828 (8 weeks). The presence of a porous/darker zone (arrow) around the colored center is clearly visible.
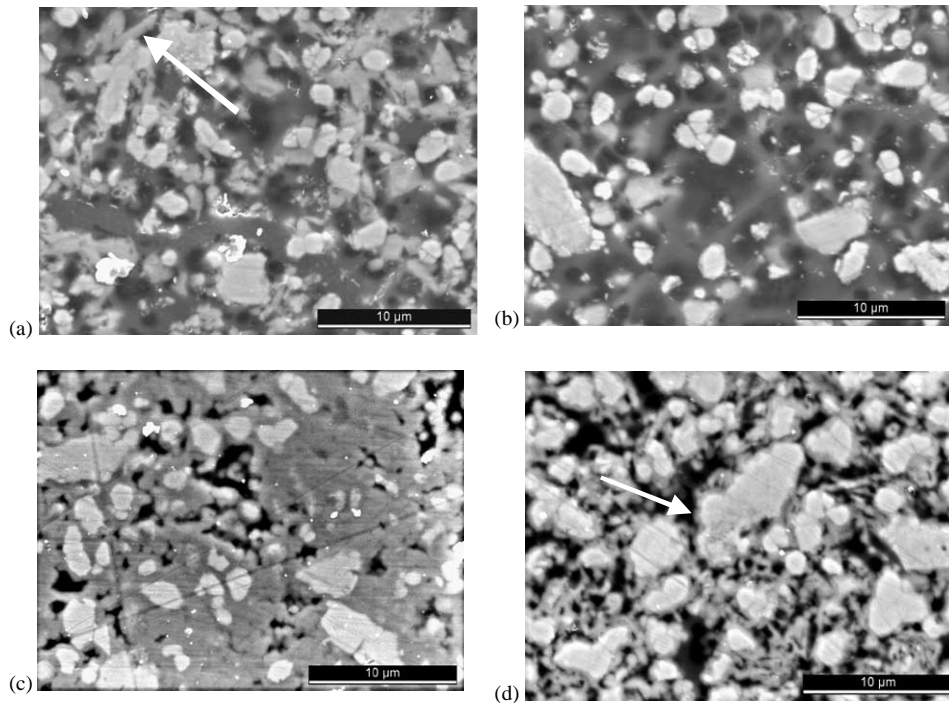
Fig. 9. SEM photos showing the microstructure of sample 828 (8 weeks): (a) away from the colored center; (b) in the porous zone adjacent to the colored center; (c) in the dense zone at the edge of the colored center; and (d) in the colored center.

832-2w, 826-4w, and 830-6w, respectively (Student's *t*-test). However, when the cement had a colored center, the Ca/P molar ratio was much larger in the colored center than in the edges. Interestingly, there was a significant decrease in the Ca/P molar ratio of the cement edge over time ($p < 0.001$). No time change of the Ca/P molar ratio could be detected in the cement center (out of the colored center).

The Ca/C weight ratio was also observed to vary (Fig. 10). The colored centers presented a much higher Ca/C weight ratio than the rest of the cement (e.g.

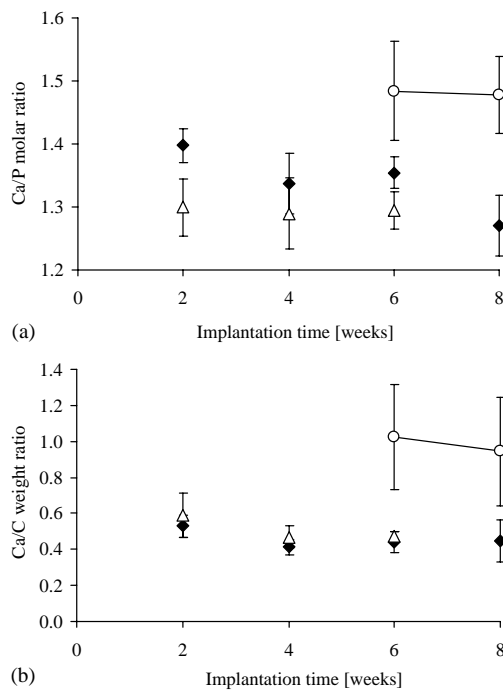Fig. 10. Ca/P molar ratio and Ca/C weight ratio in the histological sections of sheep 832 (2 weeks), 826 (4 weeks), 830 (6 weeks) and 828 (8 weeks). These EDX measurements were done: (○) in the colored center of the histological sections; (◆) at the cement edges; and (△) in the cement center, just outside the colored center. The error bars indicate 1.96 standard errors. No colored center was seen after 2 and 4 weeks.

$p < 0.0007$ for sample 830-6w), suggesting that the density of the cement in this zone was drastically increased. Additionally, magnesium was detected more frequently in the colored centers than in the edges of the cement: Mg was detected in less than 14% of the measurements done on the edges and uncolored centers, whereas Mg was detected in 6/20 (30%) and 7/15 (47%) cases in the colored center of samples 828 and 830.

The results obtained with WDS were not very different than those obtained by EDX (Table 2). For example, the values obtained for the Ca/P molar ratio were only about 0.1 smaller with WDS than with EDX. Moreover, the WDS results also demonstrated that there were large differences of composition between the different zones of the cement (Tables 2 and 3). Interestingly, no significant difference in Ca/P molar ratio and mineral content could be found between the colored center and its edge. However, the edge of the colored center was strongly enriched in magnesium (MgO/CaO = 1.53 wt%) suggesting the precipitation of a magnesium-rich phase. As a comparison, the initial MgO/CaO weight ratio of the cement was 4.2 wt%.

4. Discussion

Before implantation, the cement contained β-TCP, DCPD, β-calcium pyrophosphate (β-CPP), and sometimes DCP (Figs. 4 and 5). The presence of monetite (DCP) was probably due to an artefact of the sample preparation as no DCD was seen in implanted samples. DCPD is indeed known to easily decompose into DCP,

Table 2
Electron-microprobe WDS results

Analysis results	Colored center	Edge of colored center	Edge of matrix	Matrix
Ca/P molar ratio	1.41 (0.06)	1.42 (0.05)	1.32 (0.08)	1.19 (0.07)
MgO/CaO weight ratio (wt%)	1.14 (0.14)	1.53 (0.16)	0.64 (0.17)	0.48 (0.15)
Total content (wt%)	74.6 (4.9)	74.0 (3.9)	48.9 (9.8)	56.6 (5.6)

The standard deviation is given within parenthesis. The mineral content should be close to 100% in the absence of polymer phase. Therefore, the difference between the measured result and 100% allows one to estimate the amount of polymer, or in other words, the porosity of the cement. The terms "colored center", "edge of colored center", "edge of matrix" and "matrix" are used to describe the colored center, the dense zone at the edge of the colored center, the porous zone surrounding the edge of the colored center, and the cement matrix away from the colored center, respectively.

Table 3
Significance of the differences between different zones observed in the cement histology 828 (8 weeks)

Location	Ca/P molar ratio	MgO/CaO weight ratio (%)	Mineral content (%)
Colored center and edge of colored center	$p < 0.36$	$p < 0.002$	$p < 0.41$
Colored center and matrix edge	$p < 0.030$	$p < 5 \cdot 10^{-4}$	$p < 0.003$
Colored center and matrix	$p < 2 \times 10^{-5}$	$p < 5 \cdot 10^{-7}$	$p < 2 \cdot 10^{-5}$
Edge of colored center and matrix edge	$p < 0.022$	$p < 2 \cdot 10^{-5}$	$p < 0.002$
Edge of colored center and matrix	$p < 4 \times 10^{-5}$	$p < 2 \cdot 10^{-6}$	$p < 5 \cdot 10^{-5}$
Matrix edge and matrix	$p < 0.011$	$p < 0.065$	$p < 0.082$

The values which are not significant at the $p < 0.05$ level are underlined.

especially in acid environments [22,23]. β-CPP was present in the β-TCP powder and in the β-TCP granules used in the cement composition. Therefore, it is normal to find this phase after setting. Interestingly, the ratio of the intensity of the DCPD and β-TCP peaks was much lower in the histological sections than at time zero. One possible reason could be the partial dissolution of DCPD or different crystallization conditions in vivo. The DCPD fraction decreased over time (Fig. 5). The decrease of the DCPD content over the implantation time suggests that DCPD was either dissolved or transformed. The rather constant or increasing fractions of β-CPP and β-TCP suggest that both phases were very stable in vivo, which is in accordance with their low solubility [7].

The EDX and WDS results obtained in this study demonstrated that the colored center observed after a few weeks of implantation in the center of the cement samples contained a calcium- and magnesium-rich phase (Table 2, Fig. 10). Two explanations can be proposed for this behavior. First, there could be a selective dissolution of DCPD. As DCPD has a lower Ca/P molar ratio than β-TCP, the overall Ca/P molar ratio would be increased. This explanation is supported by the fact that DCPD has a larger solubility than β-TCP at physiological pH [7]. However, it is contradicted by the concomitant decrease of the cement porosity evidenced by the increase in Ca/C weight ratio and mineral content measured by EDX and WDS, respectively (Table 2, Fig. 10). It is also contradicted by the slower resorption rate observed beyond 2 months of implantation (Fig. 2).

The second explanation for an increase of the Ca/P molar ratio is the precipitation of a calcium-rich calcium phosphate, such as an apatite, OCP, or a whitlockite (magnesium-containing calcium phosphate) [7,24]. These reactions can occur because apatite, OCP, and whitlockite are less soluble than DCPD at physiological pH [7,24]. The presence of DCPD in close vicinity to the new precipitate could be a source of calcium and phosphate ions that could support the precipitation of additional crystals. In the latter case, the zone around the precipitation zone should become more porous and the precipitation zone should become denser. Looking at the experimental results, it appears that this explanation is in accordance with the increase in porosity measured around the colored center and with the decrease of porosity measured in the colored center (Table 2, Fig. 10). Additionally, this explanation is supported by the decrease of the cement resorption rate beyond 8 weeks of implantation (Fig. 2), and the appearance of apatite crystals, as measured by XRD (Figs. 4 and 5).

The calcium-rich phase was enriched in magnesium, suggesting the precipitation of a magnesium-rich phase or the incorporation of magnesium in the calcium-rich crystals. Unfortunately, the Mg content of the samples (Table 2) was too low to be able to detect a Mg-rich phase by XRD (whitlockite—$(Ca,Mg)_3(PO_4)_2$, JCPDS file 13-404—has a maximum peak at $d = 0.283$ nm, i.e. 2θ angle $= 31.6$). According to LeGeros et al. [25], the solution Mg/Ca ratio determines the type of calcium phosphate obtained by precipitation: apatite with incorporated Mg ions; mixture of apatite and whitlockite; mainly whitlockite, and/or Mg-containing amorphous calcium phosphate. These authors showed that whitlockite starts forming at a Mg/Ca ratio of 0.03 [25]. This value is much larger than the concentrations measured in our cements (<0.02, Table 2), suggesting that the Mg concentration present in our cement was too low to lead to the formation of whitlockite. Interestingly, an increase of the Mg content is supposed to decrease the apatite crystallinity [25]. On the SEM photos, it can be seen that the crystals present at the edge of the colored center (Fig. 9c), where the magnesium content was at a maximum, appeared to be much smaller than those present in the center of the colored zone (Fig. 9d).

Another interesting aspect is to determine the nature of the precipitated apatite. From XRD data, it appears that the peak around $d = 2.81$ Å has a lower d-value than the 100% peak of hydroxyapatite (2.78–2.79 against 2.81 Å). This suggests that the apatite is not a pure hydroxyapatite, but contains impurities. From the literature [18], it is indeed known that hydroxyapatite can easily incorporate "foreign" ions such as sodium, carbonate, hydrogenophosphate, or magnesium ions. These incorporations have a direct influence on the parameters of the lattice, and hence on the position of the XRD peaks. From EDX and WDS measurements, it appears that the zone where the apatite forms contains small, but significant amounts of magnesium, hence suggesting the formation of an apatite with magnesium substitutions. The presence of carbonate ions within the apatite cannot be determined because of the presence of the embedding polymer and the carbon coating. Sodium was not detected and hydrogenophosphate ions could not be detected. Based on these facts, it is difficult to elaborate the possible composition of the apatite. Additionally, there is hardly any XRD reference for ion-substituted apatites. There is one standard for a carbonated apatite $(Ca_{10}(PO_4)_3(CO_3)_3(OH)_2$; JCPDS File 19-272) that has a 100% peak at $d = 2.78$ Å. However, this compound is not stoichiometric and has such a large carbonate content that it is unlikely to be found in the cement. The replacement of the phosphate groups present in hydroxyapatite with hydrogenophosphate groups, for example to form a calcium deficient hydroxyapatite (CDHA; $Ca_9(PO_4)_5(HPO_4)OH$), has the tendency to increase the position of the 100% diffraction peak (from $d = 2.814$ Å for HA to $d = 2.819$ Å for CDHA—JCPDS File 46-905). Therefore, the incorporation of various ions provokes various effects. It is likely

that combinations of ionic substitutions have very complex effects. So, based on the results presented in this study, it is not possible to determine the exact composition of the precipitated apatite. However, the results indicate that an apatite is formed which contains ionic substitutions, possibly magnesium, hydrogenophosphate, carbonate and sodium, because these ions are present in the cement and in the body.

The EDX results showed that the Ca/P molar ratio measured at the cement–bone interface decreased with an increase of the implantation time, reaching after 8 weeks the values measured in the cement center. It is worth noting that the position of the interface moved over time towards the cement center because of the resorption of the cement. Taking all facts into consideration, the most likely explanation for the present results is that there was initially a gradient of Ca/P molar ratio in the cement sample. As previously mentioned, high values for the Ca/P molar ratio can be due either to the dissolution of DCPD or the precipitation of a calcium-rich phase. Here, the most likely explanation is that the cement edges were initially depleted in DCPD. Three reasons support this: (i) FTIR results showed that the cement edges had a lower DCPD/β-TCP ratio than the cement center (Fig. 7); (ii) the porosity of the cement at the edge did not vary (Fig. 10); and (iii) no new crystals were observed by SEM. When the cement was resorbed, the position of the bone–cement interface moved towards the center and the Ca/P molar ratio decreased.

The reason why the cement edges would be initially depleted in DCPD could stem from the low pH values occurring during cement setting. This explanation is somehow surprising, as the solubility of DCPD at neutral pH is lower than the equilibrium concentration of calcium and phosphate ions in vivo [7,26]. The total concentration of calcium and phosphate ions in equilibrium with DCPD in an aqueous solution at pH 7.0 is 0.90 and 1.23 mM, respectively [7]. As a comparison, these values are [Ca] = 2.42 mM and [P] = 10.1–14.3 mM in blood, and [Ca] = 2.12–2.72 mM and [P] = 2.87–4.81 mM in serum [26]. Therefore, one explanation for the selective dissolution of DCPD would be that the pH value of the solution in contact with the cement is low enough so that the solubility of DCPD at that pH value is larger than the in vivo calcium and phosphate concentrations. To meet this criterion (for calcium ions), the pH value should be below 5.8–5.9. Interestingly, the pH value occurring during the in vitro setting reaction is close to 3–4 [27]. Moreover, the pH expected at the end of the setting reaction in pure water is close to 5.9, i.e. the equilibrium pH between DCPD and β-TCP in water [27]. Therefore, assuming that this explanation is correct, this implies that the pH values in the center of the cement sample are below 6 for at least a few days. The latter explanation is based on the
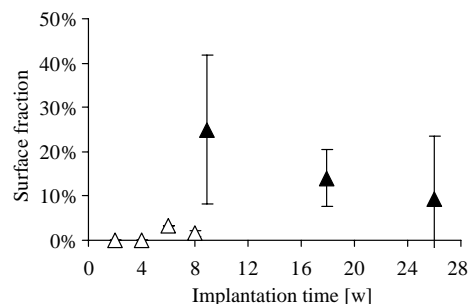

Fig. 11. Evolution of the surface fraction of the colored zone as a function of implantation time. The error bars indicate 1.96 standard errors. (▲) First in vivo study; (△) second in vivo study.

assumption that the solubility of DCPD in body fluids is not influenced by organic compounds such as proteins. In vivo, calcium and phosphate ions are likely to form complexes with proteins which could increase DCPD solubility. The extent of this effect is difficult to quantify because there is too little data in the literature on this topic. However, if this effect is large, DCPD could be soluble in body fluids, and hence spontaneously dissolve.

An interesting point that should be discussed is the position of the colored center/precipitation zone. In fact, the center of the cement is likely to be the place where the cement is the most highly saturated towards an apatite, because this is the place where there is the largest amount of DCPD and the smallest interface to the cement surroundings. Therefore, the apatite is likely to precipitate first in the center of the implanted cement samples.

Another important point is the kinetics of apatite formation. To get a better idea of the speed at which the precipitation takes place, the surface area of the colored center was measured histomorphometrically as a function of time (Fig. 11). The present experimental results show that it took 6–8 weeks of implantation to observe macroscopic amounts of apatite crystals. Additionally, the propagation of the calcium-rich zone was very fast since the average surface fraction had reached a maximum after 9 weeks (2 months). Therefore, the precipitation of apatite was not limited by diffusion, but by nucleation, possibly due to the presence of magnesium ions. Interestingly, the size of the colored zone decreased beyond 2 months of implantation, indicating that despite its transformation to a less soluble calcium phosphate, the cement remained resorbable.

In the literature, several authors reported the presence of a dense layer in a DCPD cement. For example, Frayssinet et al. [28] implanted a DCPD cement proposed by Bohner [21,29] into a defect drilled in rabbit condyles. In one sample implanted for 6 weeks a dissolution zone of thickness 100–300 μm was observed

under the material surface. This dissolution zone was edged by a densified layer less than 100 μm thick. However, these authors did not investigate the nature of this zone. Flautre et al. [10] implanted two different DCPD cements into the tibia condyle of rabbits. The cement samples were sometimes transformed into an apatite [11], and/or surrounded by a dense layer. Again, these authors did not investigate the nature of this zone. To summarize, the transformation of brushite cement into an apatite and the formation of a dense layer within the cement samples have been observed in the past. However, this is the first study analyzing these chemical changes.

5. Conclusion

The results show that the stability and resorption of DCPD cement is a complex process. The present cement formulation was observed to sustain a selective dissolution of DCPD crystals, as evidenced by FTIR and EDX. EDX results suggested that this selective dissolution took place mostly in the first 2 weeks of implantation, probably as a result of the low pH values present at early implantation times. Beyond 6–8 weeks of implantation, the center of the cement sample became denser and its Ca/P molar ratio increased. This was attributed to the transformation of DCPD crystals into apatite crystals. The appearance of a colored center in the cement samples after 6–8 weeks of implantation was correlated with a decrease of the resorption rate. Therefore, the key to keep a large resorption rate is to prevent the transformation of DCPD into a poorly soluble phase, such as an apatite. The occurrence of the latter transformation and the low amounts of Mg present in the cement after several weeks of implantation suggest that the amount of magnesium present in the cement composition was either not sufficient or not released at the right speed to prevent DCPD conversion. However, despite the transformation of DCPD into a less soluble calcium phosphate, the amount of DCPD that was transformed remained low and the apatite resulting from this transformation was still resorbable. Furthermore, due to the presence of resorbable β-TCP particles in the transformed cement matrix, the overall resorption rate of this brushite cement was still superior to that of apatite cements.

This study shows that the combination of EDX, FTIR and XRD is an excellent tool to identify compositional changes in DCPD cements. However, the easiest way to estimate the transformation of DCPD into a poorly soluble calcium-rich phase is to stain the histological sections with toluidine blue: a blue color is typical for DCPD, a violet color indicates the presence of a calcium-rich phase.

References

[1] Brown WE, Chow LC. Dental restorative cement pastes. US Patent No. 4518430, 1985.

[2] Constantz BR, Ison IC, Fulmer MT, Poser RD, Smith ST, VanWagoner M, Ross J, Goldstein SA, Jupiter JB, Rosenthal DI. Skeletal repair by in situ formation of the mineral phase of bone. Science 1995;267:1796–9.

[3] Lemaître J, Mirtchi AA, Mortier A. Calcium phosphate cements for medical use: state of the art and perspectives of development. Silic Ind 1987;9–10:141–6.

[4] Driessens FCM, Planell JA, Gil FJ. Calcium phosphate bone cements. In: Wise DL, Trantolo DJ, Altobelli DE, Yaszemski MJ, Cresser JD, Schwartz ER, editors. Encyclopedic handbook of biomaterials and bioengineering, Part B, vol. 2. New York: Marcel Dekker, 1995. p. 855–77.

[5] Lemaître J. Injectable calcium phosphate hydraulic cements: new developments and potential applications. Innov Tech Biol Med 1995;16(1):109–20.

[6] Bohner M. Calcium orthophosphates in medicine: from ceramics to calcium phosphate cements. Injury 2000;31:SD37–47.

[7] Vereecke G, Lemaître J. Calculation of the solubility diagrams in the system $Ca(OH)_2–H_3PO_4–KOH–HNO_3–CO_2–H_2O$. J Cryst Growth 1990;104:820–32.

[8] Munting E, Mirtchi AA, Lemaître J. Bone repair of defects filled with a phosphocalcic hydraulic cement: an in vivo study. J Mater Sci Mater Med 1993;4:337–44.

[9] Ohura K, Bohner M, Hardouin P, Lemaître J, Pasquier G, Flautre B. Resorption of, and bone formation from, new b-tricalcium phosphate-monocalcium phosphate cements: an in vivo study. J Biomed Mater Res 1996;30:193–200.

[10] Flautre B, Delecourt C, Blary M-C, Van Landuyt P, Lemaître J, Hardouin P. Volume effect on biological properties of a calcium phosphate hydraulic cement: experimental study in sheep. Bone 1999;25(2):35S–9S.

[11] Penel G, Leroy N, Van Landuyt P, Flautre B, Hardouin P, Lemaître J, Leroy G. Raman microspectrometry studies of DCPD cement: in vivo evolution in a sheep model. Bone 1999;25(2):81S–4S.

[12] Constantz BR, Barr BM, Ison IC, Fulmer MT, Baker J, Mckinney L, Goodman SB, Gunasekaren S, Delaney DC, Ross J, Poser RD. Histological, chemical, and crystallographic analysis of four calcium phosphate cements in different rabbit osseous sites. J Biomed Mater Res (Appl Biomater) 1998;43:451–61.

[13] Bohner M, Matter S. Brushite hydraulic cement stabilized with a magnesium salt. PCT/CH99/00595, Publication number WO 01/41824.

[14] Rousseau S, Lemaître J, Bohner M, Frei C. Long-term aging of brushite cements in physiological conditions: an in vitro study. GRIBOI, Shangai, March 14–17, 2002.

[15] Apelt D. In vivo Studie zweier injizierbarer Kalzium Phosphat Zemente; histologische und histomorphometrische Evaluation. Ph.D. Thesis, Veterinary Surgery, University of Zurich, Zurich, Switzerland, 2002.

[16] Apelt D, Theiss F, El-Warrak AO, Zlinszky K, Bettschart-Wolfisberger R, Bohner M, Matter S, Auer JA, von Rechenberg B. In vivo behavior of three different injectable hydraulic calcium phosphate cements. Biomaterials, submitted for publication.

[17] Theiss F, Apelt D, Brand B, Bohner M, Frei C, Auer JA, von Rechenberg B. Biocompatibility and resorption of a new brushite calcium phosphate cement, in preparation.

[18] Elliott JC. Mineral, synthetic and biological carbonate apatites. In: Elliott JC, editor. Structure and chemistry of the apatites and other calcium orthophosphates. Amsterdam: Elsevier, 1994. p. 191–304.

[19] Petschick R. MacDiff 4.0.6. software manual. Frankfurt am Main: Johann Wolfgang Goethe-Universität, 1999. 57pp.

[20] Pouchou JL, Pichoir F. Un nouveau modèle de calcul pour la microanalyse quantitative par spectrométrie de rayons X. La Recherche Aérospatiale 1984;3:167–92.

[21] Bohner M, Lemaître J, Ring T. Effects of sulfate, pyrophosphate, and citrate ions on the physicochemical properties of cements made of β-tricalcium phosphate–phosphoric acid–water mixtures. J Am Ceram Soc 1996;79:1427–34.

[22] Kosar-Grasic B, Purgaric B, Füredi-Milhofer H. Precipitation of calcium phosphates from electrolyte solutions. J Inorg Nucl Chem 1978;40:1877–80.

[23] Martin RI, Brown PW. Phase equilibria among acid calcium phosphates. J Am Ceram Soc 1997;80(5):1263–6.

[24] Rowles SL. The precipitation of whitlockite from aqueous solution. Bull Soc Chim Fr 1968;1797–802.

[25] LeGeros RZ, Daculsi G, Kijkowska R, Kerebel B. The effect of magnesium on the formation of apatites and whitlockites. In: Itokawa Y, Durlach J, editors. Magnesium in health and disease. London: John Libbey, 1989. p. 11–9.

[26] Turitto V, Slack SM. Blood and related fluids. In: Black J, Hastings G, editors. Handbook of biomaterial properties. London: Chapman & Hall, 1998. p. 117.

[27] Bohner M, Van Landuyt P, Merkle HP, Lemaître J. Composition effects on the pH of a hydraulic calcium phosphate cement. J Mater Sci Mater Med 1997;8:675–81.

[28] Frayssinet P, Gineste L, Conte P, Fages J, Rouquet N. Short-term implantation effects of a DCPD-based calcium phosphate cement. Biomaterials 1998;19:971–7.

[29] Bohner M. Propriétés physico-chimiques et ostéogéniques d'un biociment hydraulique à base de phosphates de calcium. Ph.D. Thesis, Swiss Federal Institute of Technology, Lausanne, Switzerland, 1993.